Colorimetric analysis of soils using flatbed scanners.

Journal:	*European Journal of Soil Science*
Manuscript ID	EJSS-324-15.R2
Manuscript Type:	Original Manuscript
Date Submitted by the Author:	02-Dec-2016
Complete List of Authors:	Kirillova, Nataliya; Moscow State University named after Lomonosov M.V., Soil Science Faculty Kemp, David; University of Aberdeen, Old Aberdeen, AB24 3UE, UK, School of Geosciences Artemyeva, Zinaida; V.V. Dokuchaev Soil Science Institute
Keywords:	soil colour, Scanner, calibration, Colorimetric, Spectrophotometer, Munsell colour chart

Colorimetric analysis of soil with flatbed scanners

N.P. KIRILLOVA[a], D.B. KEMP[b] & Z.S. ARTEMYEVA[c]

[a] *Soil Science Faculty, Moscow State University, Leninskie gory, Moscow, 119991 Russia,* [b] *School of Geosciences, University of Aberdeen, Old Aberdeen, AB24 3UE, UK, and* [c] *V.V. Dokuchaev Soil Science Institute, Pyzhevskii 7, bld. 2, Moscow, 119017 Russia*

Correspondence: N.P. Kirillova. E-mail: *npkirillova@soil.msu.ru*

Running title: Colorimetric analysis of soil with scanners

Summary

Colour is an important physical property in the characterization of soil type, and the description of soil profiles. Quantitative data from spectrophotometers and colorimeters have been used in soil research for this purpose, but semi-quantitative Munsell colour description remains the main method of soil colour evaluation. Low-cost digital devices (cameras and scanners) could largely replace the semi-quantitative assessment of colour by Munsell charts if such devices can be calibrated colorimetrically to provide accurate and reproducible data. Robust application of such tools, however, requires standardized light sources, which precludes the use of digital cameras as viable devices for use in the field. Flatbed scanners, on the other hand, enable 2-D imaging by a contact method under consistent lighting conditions. Power can be provided to such scanners through a USB port by a laptop computer, and so can be used as viable devices in the field. In this study, we explored the feasibility of using flatbed scanners to derive colorimetrically accurate images and data from a set of 161 soil samples. The efficacy of our approach was tested with two low-cost scanners, and included analysis of two commercial colour charts, six printed colour charts and three editions of the Munsell Soil Colour chart to assess the optimum methods of colorimetric calibration. For both scanners tested, we found that accurate colour characterization could be achieved for >95% of the soil samples studied (i.e. with colour errors barely perceptible by the human eye). These results illustrate the merit and efficacy of this rapid and low cost approach for soil colour evaluation.

Keywords: soil colour, calibration, spectrophotometer, Munsell colour chart

Highlights

- Can soil colour be measured accurately with commercial scanners?

- Scanners can replace semi-quantitative Munsell chart comparison or spectrophotometers
- With careful calibration, scanners can be used to measure soil colour
- Colour can be measured with an accuracy close to that achievable with spectrophotometers

Introduction

The physical characterization of soil horizons based on colour is a key diagnostic method in the description of soil profiles, and has been integrated into diagnostic keys such as the World Reference Base for Soil Resources and Russian classifications (WRB, 2014; CDSRS, 2004; FGRS, 2008). For *in situ* analysis, the Munsell colour system has been the primary qualitative or semi-quantitative means to describe soil colour (e.g. Melville & Atkinson, 1985; Viscarra Rossel *et al*., 2006; Gómez-Robledo *et al*., 2013). At the same time, the main quantitative way to describe colour in soil science is through the CIE (Commission internationale de l'éclairage) *L*a*b** system (e.g. Viscarra Rossel *et al*., 2006). In this colour space system, the colour coordinates (*a**, *b**) are separated from the lightness (*L**) coordinate (e.g. Wyszecki & Stiles, 2001). This feature of the *L*a*b** system is potentially valuable to soil scientists because it facilitates comparison of wet and dry soil. This is because moisture content affects the lightness most strongly, whereas it has less effect on *a** and *b** chromatic values (e.g. Shields *et al*., 1968). This colour system is also perceptually more uniform than, for instance, RGB (red, green, blue) colour, and hence uniform changes in *L*a*b** correspond to uniform changes in colour perceived by the human eye.

The use of portable devices to determine soil colour in the field enables objective characterization of colour on point samples, for example with spectrophotometers (e.g.

Barrett, 2002; Baibekov *et al*., 2007). To evaluate the colour of extended surfaces (2-D measurements), techniques have been developed with contactless digital devices (i.e. digital cameras). Nevertheless, accurate implementation of these methods demands the use of standardized and consistent light sources, therefore the methods are ill-suited to field use (e.g. Gomez-Robledo *et al*., 2013). For colour evaluation of extended surfaces in the field, flatbed scanners are promising because the method provides 2-D imaging by a contact method, and under consistent lighting conditions. Moreover, they are viable field devices because modern flatbed scanners can obtain power solely through a USB port when used in combination with a laptop computer. Previously, Kostenko (2009) used a low-cost flatbed scanner to acquire digital images of soil samples in the RGB colour system, but stopped short of analysing the recorded data quantitatively against spectrophotometric measurements. Flatbed scanners have been used previously for colorimetric characterization of rocks and sediments (Kemp, 2014), and for the accurate assessment of colour in fine art painting (Hardeberg, 2001).

In this study, we explore the feasibility of using flatbed scanners to derive colorimetrically accurate images and data of soil samples, and we assess the suitability of the method as a diagnostic tool for soil characterization. To do this, we undertook a series of characterization and calibration steps to optimize the colorimetric accuracy of two commercially available flatbed scanners. The basic principle underlying our approach was to characterize and calibrate scanners using a variety of colour charts containing known (spectrophotometrically analyzed) colours. We tested the accuracy of these calibrations by analysing a set of 161 spectrophotometrically measured soil samples.

Materials and Methods

Scanners

For this study, we used two flatbed scanners: an Epson v10 (Seiko Epson Corp., Japan) and a Canon LiDE220 (Canon Inc., Japan). For the Epson v10, the scanning element is a colour CCD (charge coupled device) line sensor illuminated by a white cold cathode fluorescent lamp. It is powered by AC mains power (ELG, 2015). For the Canon LiDE220 instrument, CIS (contact image sensor) technology is used and it is powered by USB (CCSL220, 2015). Contact image sensors are more adapted towards consumer quality imaging and use less power than CCDs, which makes them suitable for use in scanners that obtain power solely by USB. The light source in the Canon LiDE220 is based on a three-colour LED. Modern consumer quality scanners are designed to maximize utility, speed and design aesthetics above colorimetric accuracy, therefore both in-built software and image capture software are available with device dependent colour correction capabilities and image quality settings. To explore the effects of this processing, we chose two ways to obtain an image: without colour correction ('noCC') and with colour correction ('CC'). For the Epson v10, the image capture software used was the proprietary Epson Scan (Ver. 3.24R) used in professional mode with either (i) no colour correction (noCC) or (ii) with colour correction (CC) using the Epson sRGB ICM profile provided. For the Canon LiDE220, we used the Canon IJ Scan Utility software ScanGear (Ver. 20.0.10) with either (i) no colour correction (noCC) or (ii) colour correction (CC) with the CanonScan LiDE220 Reflective Target sRGB IEC61966-2.1. The scanners' capabilities and colorimetric accuracy were tested against measurements made with an X-Rite i1pro portable spectrophotometer device (X-Rite Europe GmbH, Regensdorf, Switzerland).

Colour charts

Characterization of the scanners was done with a variety of colour charts that each contained multiple colour chips (i.e. small squares of colour) with a wide range of colours. Two commercial colour charts IT8.7/2 (LaserSoft Imaging AG, Kiel, Germany) and ColorChecker 24 (X-Rite Inc., Michigan, USA) were used. The ColorChecker 24 was used only with the Epson v10 because it was not possible to get a sharp image on the LiDE220. Six custom colour charts were also produced that were printed on an Epson Stylus S22 (Mega Jet matte paper, Felix Schoeller GmbH, Osnabrück, Germany). The target colour range was selected to be close to the range of soil colours with different steps in lightness (L^*), redness (a^*) and yellowness (b^*). The 4.5-mm aperture of the i1pro spectrophotometer means that 360 colour chips can be fitted on one sheet of paper measuring 10 cm × 14 cm. The six sets of colour targets were produced with a common colour range of: L^*: 17.3 to 94.8, a^*: –5.3 to +28.3, and b^*: –10.2 to +34.5. In addition to these colour charts, three editions of Munsell Soil Colour charts (MSC) were also analysed: a Japanese version (in use since 1986), a USA version (1994 revised edition, in use since 2000) and a second USA version (2009 revised edition, published in 2015 and previously unused).

Soil samples

The 161 soil samples used in our study were taken from various soil horizons from the Moscow, Kursk and Far East regions of Russia. The soil types included: Retisols, Histosols, Rendzic Eutric Leptosols, Fibric Dystric Histosols, Greyic Albic Phaeozems, Histic Fluvisols, Stagnosols, Chernozems, Cambisols (WRB, 2014 classification). Samples were selected based on different soil textural classes: organic (10%), clay (7%), sandy loam (28%), clay loam (31%), silty clay loam (9%), loamy sand (8%) and sand (7%). Five percent of all samples contain carbonates (up to 89% carbonates in horizons of Histic Fluvisols).

Soil sample preparation

To produce homogenous soil samples suitable for repeat analyses, air-dried samples were crushed gently with a rubber-tipped pestle and passed through a 2-mm sieve. Water was added to the soil samples (7–10 weight %) in order to make a homogeneous mass that was put into a plastic cup with a diameter of 35 mm (depth of 10 mm, Figure 1). The addition of water prior to drying helped to cement soil particles and stopped the sample from falling to pieces when placed upside down on scanner platens. Soil was pressed manually to ensure a homogenous, flat surface. Samples were air-dried for two days to ensure stabilization of the colour. Preparation of samples in this way did not markedly change the ultimate colour of the soil samples. To demonstrate this, we measured 10 pairs of samples with initial differences in water content of 50%. After drying, the mean colour difference (ΔE_{ab^*}, see Equation (15) in Data Processing section) between pairs of samples was ~1: an imperceptible difference. Each soil cup was measured 11 times with the X-Rite i1pro spectrophotometer to determine the true colour of each soil sample (accuracy, 0.6 ΔE_{ab^*} and precision $\leq$ 0.1 ΔE_{ab^*}). For scanner analyses of these samples, about 80% of the scanned surface of each cup was extracted from the image and the average RGB values were determined. The common surface measured with the spectrophotometer was about 20–25% of the scanned measured surface.

Data processing

The aim of this study was to assess the colorimetric accuracy of the scanners, and define calibration procedures to maximize that accuracy. To do this, it is necessary to use a sequence of processing steps to allow comparison of colour measurements made on different devices and media. Scanners measure in RGB, and RGB data from the bitmap images scanned on the Epson v10 and Canon LiDE220 instruments were extracted using the program SoColEx 1.0 (Kirillova & Artemyeva, 2015).

The X-rite i1pro spectrophotometer measures the reflectance spectrum in the range 340–730 nm (i.e. visible light) and in steps of 10 nm. Conversion of the sample reflectance spectrum measured with the i1pro spectrophotometer to $L^*a^*b^*$ was implemented in two programs using standard methods: ArgyllCMS V1.6.3 (http://www.argyllcms.com) and spectral calculator spreadsheets (Lindbloom, 2010a). These programs enable the $L^*a^*b^*$ values to be calculated for the standard illuminant D50 (an approximation of natural daylight) by calculating the *XYZ* tristimulus values, which are designed to be broadly analogous to the responses of the three types of cone cells in the human eye. Characterization of the emission spectrum of the light sources of scanners was done with the i1pro spectrophotometer and the ArgyllCMS V1.6.3 software. To convert between colour spaces, for example RGB and $L^*a^*b^*$, and to compare scanner and spectrophotometer data, we used the standard conversion equations given below.

*Conversion of XYZ D50 to L*a*b**

This conversion is based on the D50 reference white, with white point coefficients: X_{wp}=0.96422, Y_{wp}=1, Z_{wp}=0.82521 (Lindbloom, 2010a).

$$L^* = 116 f_y - 16 \, , \quad (1)$$

$$a^*=500(f_x-f_y)\ , \tag{2}$$

$$b^*=200(f_y-f_z)\ , \tag{3}$$

where

$$f_x=\begin{cases}\sqrt[3]{x_{\mathrm{wp}}} & x_{\mathrm{wp}}>\varepsilon\\ \dfrac{\kappa x_{\mathrm{wp}}+16}{116} & x_{\mathrm{wp}}\le\varepsilon\end{cases}\ , \tag{4}$$

$$f_y=\begin{cases}\sqrt[3]{y_{\mathrm{wp}}} & y_{\mathrm{wp}}>\varepsilon\\ \dfrac{\kappa y_{\mathrm{wp}}+16}{116} & y_{\mathrm{wp}}\le\varepsilon\end{cases}\ , \tag{5}$$

$$f_z=\begin{cases}\sqrt[3]{z_{\mathrm{wp}}} & z_{\mathrm{wp}}>\varepsilon\\ \dfrac{\kappa z_{\mathrm{wp}}+16}{116} & z_{\mathrm{wp}}\le\varepsilon\end{cases} \tag{6}$$

and ε=0.008856 and κ=903.3 are constants

$$x_{\mathrm{wp}}=\frac{X}{X_{\mathrm{wp}}}, \tag{7}$$

$$y_{\mathrm{wp}}=\frac{Y}{Y_{\mathrm{wp}}} \tag{8}$$

and

$$z_{\mathrm{wp}}=\frac{Z}{Z_{\mathrm{wp}}}\ . \tag{9}$$

Conversion of XYZ D50 to RGB

The conversion to RGB is done in two steps (Lindbloom, 2010b). First, the transformation from *XYZ* (reference white D50) to *RGB* (i.e. RGB values in the nominal range 0 to 1) was done with the matrix ($\mathbf{M}^{-1}$) in Table 1. This gives linear *RGB* (*rgb*).

$$\begin{bmatrix} r \\ g \\ b \end{bmatrix} = \mathbf{M}^{-1} \begin{bmatrix} X \\ Y \\ Z \end{bmatrix}, \qquad (11)$$

The linear *rgb* values are then made nonlinear (*RGB*) by:

$$V = \begin{cases} 12.92v & v \le 0.0031308 \\ 1.055v^{1/2.4} - 0.055 & v > 0.0031308 \end{cases}, \qquad (12)$$

where *V* is *R* or *G* or *B* and *v* is *r* or *g* or *b*.

*Conversion of RGB to L*a*b**

The RGB values from the scanners were transformed to *L*a*b** by *XYZ* to compare with values measured with the spectrophotometer. An *RGB* colour, whose components are in the nominal range 0 to 1, is converted to *XYZ* in two steps (Lindbloom, 2010b). First, the *RGB* channels are made linear (i.e. inverse of Equation (12)):

$$v = \begin{cases} V/12.92 & V \le 0.04045 \\ ((V + 0.055)/1.055)^{2.4} & V > 0.04045 \end{cases}. \qquad (13)$$

Transformation from Linear *rgb* to *XYZ* (reference white D50) was done with the matrix (**M**) in Table 2 (Lindbloom, 2010b) as follows:

$$\begin{bmatrix} X \\ Y \\ Z \end{bmatrix} = \mathbf{M} \begin{bmatrix} r \\ g \\ b \end{bmatrix}. \qquad (14)$$

Final conversion to $L^*a^*b^*$ is then done with Equations (1–9).

Example of transformation of scanner RGB data to $L^*a^*b^*$

Let us transform the RGB colour coordinates R=100 G=80, B=10, measured on a scanner, to $L^*a^*b^*$:

1. Transform measured RGB components into the nominal range [0, 1] to get *RGB*:

$R = 100/255 = 0.3922,$

$G = 80/255 = 0.3137,$

$B = 10/255 = 0.0392.$

2. Transform *RGB* to *rgb* according to Equation (13):

$R > 0.04045$, so

$r = ((0.3922+0.055)/1.055)^{2.4} = 0.1274,$

$G > 0.04045$, so

$g = ((0.3137+0.055)/1.055)^{2.4} = 0.0802,$

B<0.04045, so

$b = 0.0392/12.92 = 0.0030.$

3. Transform *rgb* to *XYZ* according to Equation (14):

$X = r \times 0.4361 + g \times 0.3851 + b \times 0.1431,$

$Y = r \times 0.22251 + g \times 0.7169 + b \times 0.0606,$

$Z = r \times 0.0139 + g \times 0.0971 + b \times 0.71423,$

therefore:

X=0.1274×0.4361+0.0802×0.3851+0.0030×0.1431=0.0869,

Y=0.1274×0.2225+0.0802×0.7169+0.0030×0.0606=0.0860,

Z=0.1274×0.0139+0.0802×0.0971+0.0030×0.7142=0.0117.

4. Transform *XYZ* to x_{wp}, y_{wp}, z_{wp}:

$x_{wp} = X/X_{wp}$, where $X_{wp} = 0.96422$, according to Equation (7)

$x_{wp} = 0.0869/0.96422 = 0.0901,$

$y_{wp} = Y/Y_{wp}$, where $Y_{wp} = 1$, according to Equation (8)

$y_{wp} = 0.0860/1 = 0.0860,$

$z_{wp} = Z/Z_{wp}$, where $Z_{wp} = 0.82521$, according to Equation (9)

$z_{wp} = 0.0117/0.82521 = 0.0142.$

5. Transform x_{wp}, y_{wp}, z_{wp} to f_x, f_y, f_z:

$x_{wp} = 0.0901 > \varepsilon$, where $\varepsilon = 0.0088560$, and so according to Equation (4)

$f_x = (x_{wp})^{1/3} = (0.0901)^{1/3} = 0.4483,$

$y_{wp} = 0.0860 > \varepsilon$,

and so according to Equation (5)

$f_y = (y_{wp})^{1/3} = (0.0860)^{1/3} = 0.4415,$

$z_{wp} = 0.0142 > \varepsilon,$

and so according to Equation (6)

$f_z = (z_{wp})^{1/3} = (0.0142)^{1/3} = 0.2423.$

6. Transform f_x, f_y, f_z to L^*, a^*, b^*:

$L^* = 116 f_y - 16$, according to Equation (1)

$L^* = 116 \times 0.4415 - 16 = 35.21,$

$a^* = 500(f_x - f_y)$, according to Equation (2)

$a^* = 500 \times (0.4483 - 0.4415) = 3.43,$

$b^* = 200(f_y - f_z)$, according to Equation (3)

$b^* = 200 \times (0.4415 - 0.2423) = 39.84.$

Example of transformation of XYZ to RGB

Let us transform the *XYZ* tristimulus values X=0.0869, Y=0.0860, Z=0.0117, derived from the i1pro spectrophotometer spectrum, to RGB:

1. Transform *XYZ* to *rgb* according to Equation (11):

$r = X \times 3.1339 - Y \times 1.6169 - Z \times 0.4906,$

$g = -X \times 0.9788 + Y \times 1.9161 + Z \times 0.03345,$

$b = X \times 0.07195 - Y \times 0.2290 + Z \times 1.4052.$

therefore:

$r = 0.0869 \times 3.1339 - 0.0860 \times 1.6169 - 0.0117 \times 0.4906 = 0.1275,$

$g = -0.0869 \times 0.97884 + 0.0860 \times 1.9161 + 0.0117 \times 0.03345 = 0.0801.$

$b = 0.0869 \times 0.07195 - 0.0860 \times 0.2290 + 0.0117 \times 1.4052 = 0.0030.$

2. Transform *rgb* to *RGB* (in nominal range 0 to 1) according to Equation (12):

$r = 0.1275 > 0.0031308$, so

$R = 1.055 \times r^{1/2.4} - 0.055 = 1.055 \times (0.1275)^{1/2.4} - 0.055 = 0.3922,$

$g = 0.0801 > 0.0031308$, so

$G = 1.055 \times g^{1/2.4} - 0.055 = 1.055 \times (0.0801)^{1/2.4} - 0.055 = 0.3137,$

$b = 0.0030 < 0.0031308$, so

$B = 12.92 \times b = 12.92 \times 0.0030 = 0.0392.$

1. Transform *RGB* components into the range [0, 255] to get RGB:

R = 0.3922 × 255 = 100,

G = 0.3137 × 255 = 80,

B = 0.0392 × 255 = 10.

Colour difference calculation

The processing steps above enable colours measured on both the scanners and the i1pro spectrophotometer to be compared quantitatively. To quantify differences in the colours measured on these devices, we can use the CIELAB colour difference formula. This formula calculates the absolute colour difference in terms of the Euclidean distance in the position of the L^*, a^* and b^* values (ΔE_{ab^*}) for the D50 reference illuminant (Wyszecki & Stiles, 2001):

$$\Delta E_{ab^*} = [(L^*_{\text{true}} - L^*_{\text{scanned}})^2 + (a^*_{\text{true}} - a^*_{\text{scanned}})^2 + (b^*_{\text{true}} - b^*_{\text{scanned}})^2]^{1/2}, \quad (15)$$

where L^*_{true}, a^*_{true} and b^*_{true} are the values calculated after analysis with the spectrophotometer, and L^*_{scanned}, a^*_{scanned} and b^*_{scanned} are the values calculated from scanned images. A more recent colour difference formula (the CIEDE2000 colour difference formula) has been designed to overcome shortcomings in the perceptual uniformity of the CIELAB measure (e.g. Sharma *et al*., 2005). It is computationally more involved, but is implemented in this study to aid comparison using Excel spreadsheets provided by Sharma *et al.* (2005).

Results

Correlation between spectrophotometer and scanned RGB values

To obtain an accurate estimate of soil colour measured by a scanner, it is necessary to study the effects of the scanner's settings on the scanned RGB values. The relation between the scanned RGB values and spectrophotometrically derived RGB values is determined by the following properties: the initial sample colour range (the colour scheme of the samples), scanner type and colour processing mode. With a small colour range (i.e. grey colour chart) and no colour correction (noCC), the relation between the scanned and spectrophotometrically determined RGB is described well by a second-order (quadratic) polynomial with large correlation coefficients and small RMSE (root mean square error) for both scanners (Figures 2 and 3). A greater colour range leads to the considerable deterioration in the strength of the correlation between scanned and true values, and the RMSE increases for R and B by a factor of almost 4 (Figures 4 and 5). Thus, the RSME increases with the number of colour chips when no colour correction is used (Table 3). When the scanning mode was set to use the internal colour correction (CC) offered by both scanners, the relation has a linear form (Figures 6–11). Increasing the colour range (i.e. number of colour chips) still leads to a deterioration in the strength of correlation, but less so than when no colour correction was used (approximately two-fold increase in RMSE, compared with a four-fold increase in measurements made with no colour correction, Table 4). Colour correction, therefore, offers better potential for accurate colorimetric characterization.

Calibration: correction of scanned RGB values

Scanning with colour correction means that the procedure of RGB correction becomes simplified. This is because the results presented above show that the relation between the scanned and true RGB values is linear when colour correction (CC) is used for both scanners (Figures 6–11, Table 4). Therefore, we can obtain the corrected (i.e. calibrated) RGB values with the linear equations that describe the relation between the scanned and measured RGB values as follows:

$$R(G,B)_{\mathrm{corrected}} = mR(G,B)_{\mathrm{scanned}} + b, \qquad (16)$$

where $R(G,B)_{corrected}$ are corrected values, $R(G,B)_{scanned}$ are scanned values, m and b are the coefficients of the linear equations.

Colorimetric calibration and accuracy

Following the procedures outlined above, we used the colour charts introduced earlier to define the correlations and calibrations between scanned and true (spectrophotometrically measured) colours. We then quantified the colorimetric accuracy of these calibrations by measuring samples from our soil sample set. The general scheme to calculate corrected $L^*a^*b^*$ values from scanned RGB values is presented in Figure 12. We calculated the coefficients of the linear equations that describe the relation between scanned and true RGB values with the various colour charts discussed earlier. In addition to the six custom charts, two commercial charts and the three Munsell colour charts mentioned, we also used a subset of the soil samples for calibration.

Our results show that the best colorimetric accuracy was achieved when soil samples were used as calibration targets (Table 5). Ten soil samples were determined to be a sufficient number to obtain an average ΔE_{ab^*} of <2, and 96–98% of samples gave a value of ΔE_{ab^*} <3. A ΔE_{ab^*} colour difference of <3 is hardly perceptible to a human observer. Paper charts could be used, but for the Epson v10 only. Calibration with both the colour paper set and ‘neutral' paper set (i.e. predominantly black–grey–white chips) meant that >75% of the samples had a mean ΔE_{ab^*} <3. It is particularly interesting that the neutral paper (45 chips) showed very good results (95.2% of samples with ΔE_{ab^*} <3 for the Epson v10), but for the LiDE220 this chart had only 13.3% of colours with ΔE_{ab^*} <3, and indeed no colour set provided acceptable results. Coefficients of linear equations for the paper charts and soil target set are similar for the Epson (Table 6), but more different for the LiDE220. To understand this phenomenon, we analysed soil spectra (Figure 13). Growth maximum of reflectance spectra (i.e. where the slope of the percent reflectance curve changes the most rapidly) is ~590 nm for paper and ~570 nm for soil. In this range, the LiDE220 has poor relative power, and it is larger at 590 nm than at 570 nm. Thus, linear coefficients for soil samples are different from paper samples.

Given their widespread use by soil scientists, and the similarity in colour with real soil, we explored the possibility of using Munsell colour charts for scanner calibration. Colour chips in three editions of the Munsell scale were analysed with the scanners and the i1pro spectrophotometer. As noted earlier, the charts were: a Japanese version from 1986, an American version from 1994 and an unused 2009 American version. This comparison provides information on how the colour characteristics of the various chips change with time. Soil scientists often use old charts, even though according to the manufacturer's recommendations the service life of the charts is ~2 years.

Our results show that the relation between the scanned and true RGB values of the Munsell charts is linear (Figures 8, 11; Table 4). However, as demonstrated by our analysis of printed scales, this linearity does not guarantee success in colorimetric characterization and accurate analysis of real soil samples (Tables 4 and 5). The main indicator is proximity of the reflectance of the pigments used for printing to the reflectance of soil pigments. According to this indicator, the charts of the Munsell scale are markedly different. We assessed these differences by comparing the mean ΔE_{ab*} values obtained with Munsell soil colour charts on the set of 161 soil samples (Table 7). The mean ΔE_{ab*} value (for all charts and all versions) for the Epson v10 scanner was less than for the LiDE220 scanner (2.41 and 2.83 respectively). The mean value for both of the used Munsell charts was somewhat worse (2.72) than for the newer, unused Munsell chart (2.40). The smallest mean value of ΔE_{ab*} for the two scanners (1.96) was for the 2.5Y (yellow hue) sheet in the Munsell book and the largest was for the

Gley 2 sheet (3.75). The best values for 2.5Y might be because of the stability of these particular pigments and how often the sheet was used. In this sense, for the most frequently used sheets (7.5 YR, 10YR: yellow–red hues) the difference between the old and new scales is greater than for the less frequently used 2.5Y sheet. The best result for soil analysis was from the Epson v10 scanner (1.15) when soil sample calibration was used. The closest to that was the 10YR sheet of the newest Munsell chart (1.30). For the LiDE220 scanner, the best result (1.41) was also with the soil samples, followed by the 5Y sheet of the newest Munsell chart (1.84).

To investigate the colour accuracy of the scanners further, we calculated the CIEDE2000 colour difference for the 161 soil samples measured with the three versions of the Munsell Colour charts. As indicated above, the CIEDE2000 formula has been shown to be a potentially better metric than ΔE_{ab*} because the CIELAB space is not as perceptually uniform as was originally intended (Sharma *et al.*, 2005). The relation between ΔE_{ab*} and CIEDE2000 is shown in Figure 14. The CIEDE2000 value is 85–86% of the ΔE_{ab*} value. Therefore, if ΔE_{ab*}<3, then it is very likely that CIEDE2000 would also be less than 3.

Taking all these results together, we find that of the non-soil colour targets used, the best results were obtained with the Munsell charts. Our results confirm that at least for some charts, however, colour characteristics do change over time because of fading of the pigment. If the chart is used for calibration in the laboratory only and not in the field, this should minimize this issue. Neutral paper colour sets with a colour range close to black–grey–white have almost the same linear coefficients as soil sample colour sets with the Epson v10. These sets provide the same mean ΔE_{ab*} <2 for all samples and ΔE_{ab*} <3 for more than 90% of soil samples (Table 5). Neutral colour paper could not be used to evaluate soil colour on the LiDE220. Its linear coefficients are very different from the coefficients calculated for soil (Table 6). Neutral colour paper provides a mean ΔE_{ab*} of 4.47 and a ΔE_{ab*} of <3 for only

13.3% of the analysed samples (Table 5). These results explain the findings of Gomez-Robledo *et al.* (2013) who noted that ΔE_{ab*} increased by more than 2 when targets were changed from Munsell colour chart to soil samples and NCS (Natural Colour System, Sweden) samples (Gómez-Robledo *et al.*, 2013).

For five of the 161 soil samples, the colour calibration was not accurate (i.e. ΔE_{ab*} greater than 3). In those cases, we have identified two main reasons. The first relates to the surface roughness of the soil samples, which led to heterogeneities in the colour of the sample surface. Repeated sample preparation with smoothing resulted in obtaining re-measured samples with a ΔE_{ab*}<3. A further reason identified for three of the five samples was that these samples contained considerable sand content. In this case, the discrepancy is related to the pigments associated with the colour of the minerals in the sand. When sand from the same soil profile contained more Fe-hydroxides, the colours of the mineral component were masked and the ΔE_{ab*} of the sample became <3.

Conclusions

Our study has shown that with the use of widely available and low-cost commercial flatbed scanners, $L*a*b*$ colour measurements can be obtained that are close to those measured with a more expensive point sampling spectrophotometer. Absolute colour differences of ΔE_{ab*}<3 are achievable with our methods. This difference is hardly perceptible to a human observer. A scanning mode with device-specific colour correction provided acceptable results, with mean ΔE_{ab*} <2 for all samples and ΔE_{ab*} <3 for more than 95% of the soil samples studied when 10 soil samples were used as a calibration set (Table 5). Our results have also shown that Munsell colour charts can be used to characterize scanners colorimetrically. This is encouraging given their popular use amongst soil scientists. We found that a Munsell chart used for scanner calibration can provide a mean ΔE_{ab*} of <2, with ΔE_{ab*} <3 for more than 90% of the samples tested (Table 5).

Acknowledgements

This work was supported by the Russian Science Academy Presidium (2015). The CIEDE2000 calculation of Sharma *et al*. (2005) was made available from spreadsheets from these authors.

References

ArgyllCMS V1.6.3 [WWW document]. URL https://www.argyllcms.com [accessed on 18 October 2015].

Baibekov, R.F., Savich, V.I., Egorov, D.N. & Hesam Mousa. 2007. Evaluation of soil colour under field conditions by using Gretag Macbeth Eye-One Photo device. *Izvestiya of Timiryazev Agricultural Academy*, **4**, 23–28 (in Russian).

Barrett, L.R. 2002. Spectrophotometric color measurement in situ in well drained sandy soils. *Geoderma*, **108**, 49–77.

CCSL220, 2015. Canon CanoScan LiDE220. CanoScan Flatbed Photo & Document Scanners. Product Specification. [WWW document]. URL https://www.canon.co.uk/scanners/flatbed-scanners/canoscan_lide_220 [accessed on 18 October 2015].

CDSRS, 2004. *Classification and Diagnostic System of Russian Soils*. Oikumena, Smolensk (in Russian).

ELG, 2015. Epson v10 on line guide. [WWW document]. URL https://support.epson-europe.com/onlineguides/en/perfv10/html/specs_2.htm [accessed on 18 October 2015].

FGRS, 2008. *Field Guide for Russian Soils*. Dokuchaev Soil Institute, Moscow (in Russian).

Gómez-Robledo, L., López-Ruiz, N., Melgosa, M., Palma, A.J., Capitán-Vallvey, L.F. & Sánchez-Marañón, M. 2013. Using the mobile phone as Munsell soil-colour sensor: an experiment under controlled illumination conditions. *Computers and Electronics in Agriculture*, **99**, 200–208.

Hardeberg, J.Y. 2001. *Acquisition and Reproduction of Color Images*. [WWW document]. URL https://www.dissertation.com/library/11213 50a.html [accessed on 10 March 2015]. USA. 2001. ISBN: 1-58112-135-0

Kemp, D.B. 2014. Colorimetric characterisation of flatbed scanners for rock/sediment imaging. *Computers & Geosciences*, **67**, 69–74.

Kirillova, N.P. & Artemyeva, Z.S. *RF Patent 2015618613*, 12.08.2015. Russia, Moscow.

Kostenko I. V. 2009. Scanning study of the optical parameters of sandy soddy-Steppe soil samples from the Southern Ukraine. *Eurasian Soil Science*, **42**, 1012–1020.

Lindbloom B. 2010a. *Spectral Calculator*. [WWW document]. URL https://www.brucelindbloom.com/downloads/SpectralCalculator10nm.xls.zip [accessed on 20 November 2016].

Lindbloom B. 2010b. *Useful Color Equations*. [WWW document]. URL https://www.brucelindbloom.com/Eqn_*XYZ*_to_Lab.html [accessed on 20 November 2016].

Melville, M.D. & Atkinson, G. 1985. Soil colour: its measurement and its designation in models of uniform colour space. *Journal of Soil Science*, **36**, 495–512

Sharma, G., Wu, W. & Dalal, E. 2005. The CIEDE2000 color-difference formula: Implementation notes, supplementary test data, and mathematical observations. *Color Research and Applications*, **3**, 21–30.

Shields, J.A., Paul, A., Arnaud, R.J. & Head, W.K. 1968. Spectrophotometric measurement of soil color and its relationship to moisture and organic matter. *Canadian Journal of Soil Science*, **48**, 271–280.

Viscarra Rossel, R.A., Minasny, B., Roudier, P. & McBratney, A.B. 2006. Colour space models for soil science. *Geoderma*, **133**, 320–337.

WRB 2014. *World Reference Base for Soil Resources. International Soil Classification System for Naming Soils and Creating Legends for Soil Maps*. IUSS Working Group. World Soil Resources Reports No 106. FAO, Rome.

Wyszecki, G. & Stiles, W.S. 2001. *Color Science: Concepts and Methods, Quantitative Data and Formulae*, Second Edition. Wiley, New York, NY.

Figure captions

Figure 1. A soil sample cup prepared for scanning: (a) scanned image and (b) selected part used for extraction of RGB values

Figure 2. Scanned RGB values determined on an Epson v10 scanner (noCC) plotted against true (i1pro measured) RGB values for: (a) R, (b) G and (c) B. Range of true values: *L**, 9.5 to 90.4; *a**, −0.6 to 6.1 and *b**, −10 to 5.7; *N*=69. Second-order polynomial (quadratic) equations are also given.

Figure 3. Scanned RGB values determined on a Canon LiDE220 scanner (noCC) plotted against true (i1pro measured) RGB values for: (a) R, (b) G and (c) B. Range of true values: *L**, 9.05 to 90.4; *a**, −0.6 to 6.1 and *b**, −10 to 5.7; *N*=69. Secondorder polynomial (quadratic) equations are also given.

Figure 4. Scanned RGB values determined on an Epson v10 scanner (noCC) plotted against true (i1pro measured) RGB values for: (a) R, (b) G and (c) B. Range of true values: *L**, 8.9 to 95.5; *a**, −49.5 to 70.4; *b**, −68.5 to 84.0; *N*=2037. Second-order polynomial (quadratic) equations are also given.

Figure 5. Scanned RGB values determined on a Canon LiDE220 scanner (noCC) plotted against true (i1pro measured) RGB values for: (a) R, (b) G and (c) B. Range of true values: *L**: 8.9 to 90.4; *a**: −49.5 to 70.4; *b**: −68.5 to 84.6; *N*=2012. Secondorder polynomial (quadratic) equations are also given.

Figure 6. Scanned RGB values determined on an Epson v10 scanner (CC) plotted against true (i1pro measured) RGB values for: (a) R, (b) G and (c) B. Range of true values: *L**, 9.5 to 90.4; *a**, −0.6 to 6.1; *b**, −10 to 5.7; *N*=69. Linear equations are also given.

Figure 7. Scanned RGB values determined on an Epson v10 scanner (CC) plotted against true (i1pro measured) RGB values for: (a) R, (b) G and (c) B. Range of true values: L^*, 8.9 to 95.5; a^*, −49.5 to 70.4; b^*, −68.5 to 84.0; N=2037. Linear equations are also given.

Figure 8. Scanned RGB values determined on an Epson v10 scanner (CC) plotted against true (i1pro measured) RGB values for: (a) R, (b) G and (c) B. Colours are from Munsell Soil Colour charts: 10R, 2.5YR, 5YR, 7.5YR, 10YR, 2.5Y, 5Y; USA version, revised 2009. Range of target true values: L^*, 20.5 to 82.8; a^*, 0 to 36.3; b^*, 3.4 to 57.5; N=238. Linear equations are also given.

Figure 9. Scanned RGB values determined on a Canon LiDE220 scanner (CC) plotted against true (i1pro measured) RGB values for: (a) R, (b) G and (c) B. Range of true values: L^*, 9.5 to 90.4; a^*, −0.6 to 6.1; b^*, −10 to 5.7; N=69. Linear equations are also given.

Figure 10. Scanned RGB values determined on a Canon LiDE220 scanner (CC) plotted against true (i1pro measured) RGB values for: (a) R, (b) G and (c) B. Range of true values: L^*, 8.9 to 90.4; a^*, −49.5 to 70.4; b^*, −68.5 to 84.6; N=2012. Linear equations are also given.

Figure 11. Scanned RGB values determined on a Canon LiDE220 scanner (CC) plotted against true (i1pro measured) RGB values for: (a) R, (b) G and (c) B. Colours are from Munsell Soil Colour charts: 10R, 2.5YR, 5YR, 7.5YR, 10YR, 2.5Y, 5Y; USA version, revised 2009. Range of target true values: L^*, 20.5 to 82.8; a^*, 0 to 36.3; b^*, 3.4 to 57.5; N=238. Linear equations are also given.

Figure 12. Flow chart of the colour coordinate linear transformations of RGB and calculation of colour difference (ΔE_{ab^*}). LAB are L^*, a^*, b^* values; XYZ are the tristimulus values

Figure 13. Relative spectral power distribution for the Epson v10 illuminant, the LiDE220 illuminant and reflectance spectra of soil and paper samples

Figure 14. The relation between ΔE_{ab}^* and CIEDE2000 measured with three versions of the

Munsell Colour charts (*N* charts=33, *N* soil samples=161): (a) Epson v10 scanner and (b) Canon LiDE220 scanner.

Table 1. The matrix of transformation from *XYZ* D50 colour coordinates to linear RGB (*rgb*) (from Lindbloom, 2010b)

Colour coordinate	*X*	*Y*	*Z*
r	3.1339	−1.6169	−0.4906
g	−0.9788	1.9161	0.03345
b	0.07195	−0.2290	1.4052

Table 2. The matrix of transformation from linear RGB (*rgb*) to *XYZ* D50 (from Lindbloom, 2010b)

Colour coordinate	*r*	*g*	*b*
X	0.4361	0.3851	0.1431
Y	0.2225	0.7169	0.06061
Z	0.01393	0.09710	0.7142

Table 3. Coefficients, standard errors (SE), the Pearson correlation coefficient (*r*) and the coefficient of determination (R^2) of the quadratic statistical model $y=ax^2+bx+c$ built to compute $RGB_{corrected}$ from $RGB_{scanned}$ (scanning mode, noCC).

Scanner	Colour chart name	Number of chips /N	Colour variable	*a*	SE*a*	*b*	SE*b*	*c*	SE*c*	*r*	R^2	RMSE
Epson v10	Paper, C, neutral &IT8.7/2 , neutral part	69	R	−0.0019	0.0001	1.40	0.0210	0.63	1.0956	0.9993	0.9986	2.34
			G	−0.0019	0.0001	1.43	0.0152	−0.22	0.7828	0.9996	0.9992	1.77
			B	−0.0014	0.0001	1.23	0.0143	10.81	0.7553	0.9996	0.9992	1.70
	Paper, C &IT8.7/2 & ColorChecker24	2037	R	−0.0024	0.0001	1.58	0.0191	−9.87	1.1216	0.9849	0.9700	8.34
			G	−0.0017	0.0001	1.38	0.0105	0.07	0.5564	0.9950	0.9900	4.51
			B	−0.0003	0.0001	1.02	0.0189	14.74	0.9850	0.9824	0.9652	8.31
LiDE220	Paper, C, neutral &IT8.7/2 , neutral part	69	R	−0.0008	0.0001	1.21	0.0178	−7.05	0.9976	0.9996	0.9993	1.69
			G	−0.0008	0.0001	1.24	0.0147	−10.98	0.8195	0.9997	0.9995	1.41
			B	−0.0004	0.0001	1.07	0.0271	5.83	1.4839	0.9990	0.9980	2.67
	Paper, C &IT8.7/2	2012	R	−0.0013	0.0001	1.40	0.0166	−22.19	1.0522	0.9917	0.9834	6.16
			G	−0.0003	0.0001	1.13	0.0132	−10.59	0.7792	0.995	0.9901	4.46
			B	0.0001	0.0001	1.00	0.0148	4.36	0.8154	0.9925	0.9851	5.41

$R(G,B)_{corrected} = aR^2(G^2,B^2)_{scanned} + bR(G,B)_{scanned} + c$

RMSE, root mean squared error.

Table 4. The linear equation coefficients (*m, b*) with standard error (SE), Pearson correlation coefficient (*r*) and the coefficient of determination (R^2) for different colour charts and scanners (scanning mode, CC).

Scanner	Colour chart name	Number of chips /N	Colour variable	*m*	SE_m	*b*	SE_b	*r*	R^2	RMSE
Epson V10	Paper, C, neutral &IT8.7/2 , neutral part	69	R	0.94	0.0067	10.57	0.9698	0.9983	0.9966	3.61
			G	1.02	0.0041	−8.01	0.6208	0.9994	0.9989	2.12
			B	0.92	0.0048	10.59	0.7083	0.9990	0.9981	2.60
	Paper, C &IT8.7/2 & ColorChecker24	2037	R	0.95	0.0016	7.30	0.2570	0.9970	0.9941	3.72
			G	1.03	0.0017	−9.62	0.2427	0.9971	0.9943	3.41
			B	0.91	0.0021	11.64	0.2562	0.9949	0.9898	4.51
LiDE220	Paper, C, neutral &IT8.7/2 , neutral part	69	R	0.99	0.0039	5.49	0.5637	0.9995	0.9989	2.03
			G	1.00	0.0054	4.50	0.7603	0.9990	0.9981	2.80
			B	0.93	0.0051	12.78	0.7257	0.9990	0.9980	2.70
	Paper, C &IT8.7/2	2012	R	0.99	0.0015	1.55	0.2308	0.9978	0.9956	3.18
			G	0.99	0.0017	−0.18	0.2242	0.9972	0.9945	3.33
			B	0.93	0.0017	13.37	0.2102	0.9965	0.9930	3.72
Epson V10	MSC, J	240	R	0.97	0.0037	11.40	0.5578	0.9983	0.9966	2.80
			G	1.05	0.0033	−9.39	0.4310	0.9988	0.9977	1.97
			B	0.98	0.0062	6.07	0.6015	0.9952	0.9904	3.32
	MSC, USA, 1994	234	R	1.01	0.0025	7.39	0.4075	0.9993	0.9985	1.90
			G	1.05	0.0048	−9.84	0.6697	0.9976	0.9952	3.11
			B	0.99	0.0039	7.21	0.4283	0.9982	0.9963	2.53
	MSC, USA, 2009	238	R	0.98	0.0027	6.44	0.4510	0.9991	0.9981	2.17
			G	1.02	0.0037	−10.44	0.5281	0.9984	0.9969	2.60
			B	0.94	0.0045	7.13	0.4956	0.9973	0.9945	3.28
	MSC, Jp	240	R	1.10	0.0039	−1.34	0.5584	0.9985	0.9971	2.59
			G	1.10	0.0042	2.92	0.4832	0.9982	0.9965	2.42
			B	1.07	0.0052	−2.21	0.4996	0.9972	0.9944	2.55
			R	1.11	0.0056	−0.24	0.8427	0.9971	0.9943	3.76

LiDE220	MSC, USA, 1994	234	G	1.09	0.0056	6.18	0.6796	0.9970	0.9939	3.52
			B	1.05	0.0039	1.24	0.4148	0.9984	0.9969	2.33
			R	1.09	0.0039	0.08	0.6009	0.9985	0.9970	2.79
	MSC, USA, 2009	238	G	1.06	0.0051	6.09	0.6185	0.9973	0.9947	3.41
			B	1.05	0.0036	−1.06	0.3775	0.9986	0.9972	2.33

$R(G,B)_{corrected}=mR(G,B)_{scanned}+b$

MSC, Munsell Soil Colour charts: 10R, 2.5YR, 5YR, 7.5YR, 10YR, 2.5Y, 5Y; Jp, Japanese version; USA, USA version 1994 revised edition; 2009 revised edition.
RMSE, root mean squared error

Table 5. Statistical summary of the differences between measured and true $L^*a^*b^*$ values of soil samples (ΔE_{ab^*}) for different calibrations (scanning mode CC).

Colour chart used for calibration	Scanner	Number soil samples measured	ΔE_{ab^*}<3 /%	ΔE_{ab^*}<6 /%	Mean ΔE_{ab^*}	st. dev. ΔE_{ab^*}	Minimum ΔE_{ab^*}	Median ΔE_{ab^*}	Maximum ΔE_{ab^*}	Skewness coefficient
ColorChecker24[a]	Epson v10	125	0	61.6	6.04	1.47	3.57	5.74	12.91	2.20
IT8.7/2 [b]	Epson v10	125	4.0	96.0	4.01	0.80	2.12	3.83	7.22	1.42
IT8.7/2[b]	LiDE220	135	0	3.0	9.47	1.54	4.24	9.45	12.70	−0.40
IT8.7/2[c], neutral part	Epson v10	125	0.8	80.8	5.48	0.81	2.60	5.50	7.95	−0.12
IT8.7/2[c], neutral part	LiDE220	135	4.4	77.8	5.10	1.00	2.30	5.05	7.76	−0.27
Paper, C[d] , colour	Epson v10	125	76.8	99.2	2.74	0.76	1.35	2.60	6.19	1.77
Paper, C[d], colour	LiDE220	135	0	0.7	9.75	1.27	5.90	9.78	12.98	−0.39
Paper, C[e], neutral	Epson v10	125	95.2	100.0	1.62	0.73	0.31	1.44	4.36	1.33
Paper, C[e], neutral	LiDE220	135	13.3	91.1	4.47	1.30	0.81	4.58	7.69	−0.44
Soil[f]	Epson v10	161	97.5	100.0	1.15	0.60	0.17	1.05	5.96	1.40
Soil[f]	LiDE220	161	96.9	100.0	1.41	0.66	0.15	1.36	5.26	0.59
MSC[g] 10YR	Epson v10	161	95.7	100.0	1.30	0.83	0.23	1.06	4.89	1.32
MSC[h] 5Y	LiDE220	161	96.3	100.0	1.84	0.55	0.66	1.83	3.49	0.37

[a] ColorChecker24, commercial colour chart, 24 chips. Colour range: L^*:17.3 to 94.8; a^*: −5.3 to 28.3; b^*: −10.2 to 34.5.

[b] IT8.7/2, commercial colour chart, 288 chips. Colour range: L^*: 8.9 to 92.5; a^*: −49.5 to 70.4; b^*: −68.5 to 84.6.

[c] IT8.7/2, commercial colour chart, 24 chips. Colour range: L^*: L^*: 8.9 to 92.5; a^*: −1.1 to 2.2; b^*: 0.4 to 6.4.

[d] Custom (C) colour chart, paper, 1725 chips. Colour range: L^*:17.3-94.8; a^*: −5.3 to 28.3; b^*: −10.2 to 34.5.

[e] Custom (C) neutral chart, paper, 45 chips. Colour range: L^*: 17.3 to 90.4; a^*: −0.6 to 2; b^*: −2.2 to 0.5.

[f] Soil samples (10). Colour range: L^*: 14.9 to 65.3; a^*: 2.0 to 19.4; b^*: 2.8 to 28.2.

[g] Munsell Colour chart, USA version, 2009 revised edition, published in 2015, Hue 5YR. Colour range: L^*: 20.5 to 82.3; a^*: 2.1 to 17.3; b^*: 4.1 to 52.5.

[h]- Munsell Colour chart, USA version, 2009 revised edition, published in 2015, Hue 5Y. Colour range: L^*: 25.5 to 82.2; a^*: 0 to 5.9; b^*: 4.1 to 57.5.

Table 6. The linear equation coefficients with standard errors (SE), Pearson correlation coefficient (r) and the coefficient of determination (R^2) for different colour chart types and scanners (scanning mode, CC).

Scanner	Colour chart name	Number of chips	Colour variable	m	SE_m	b	SE_b	r	R^2
Epson V10	Paper, C, neutral	45	*R*	0.92	0.006	14.78	0.967	0.9989	0.9979
			G	1.02	0.006	−9.03	0.881	0.9993	0.9987
			B	0.92	0.005	8.78	0.781	0.9994	0.9987
	Soil	10	*R*	0.97	0.013	10.34	1.589	0.9994	0.9985
			G	1.03	0.017	−9.39	1.886	0.9989	0.9975
			B	1.03	0.036	2.53	2.701	0.9952	0.9893
	MSC 10YR	36	*R*	0.97	0.005	8.20	0.857	0.9995	0.9990
			G	1.01	0.006	−9.54	0.855	0.9994	0.9988
			B	0.92	0.011	9.30	1.093	0.9977	0.9955
LiDE220	Paper, C, neutral	45	*R*	0.98	0.005	6.37	0.798	0.9994	0.9987
			G	0.99	0.005	7.55	0.770	0.9994	0.9988
			B	0.96	0.004	8.78	0.603	0.9996	0.9992
	Soil	10	*R*	1.08	0.025	−3.92	3.158	0.9979	0.9953
			G	1.11	0.037	−0.79	3.511	0.9956	0.9901
			B	1.04	0.041	−2.96	3.279	0.9938	0.9860
	MSC 5Y	31	*R*	1.07	0.008	1.35	1.197	0.9992	0.9984
			G	1.08	0.013	4.10	1.806	0.9976	0.9953
			B	1.05	0.010	0.35	1.024	0.9986	0.9973

$R(G,B)_{\text{corrected}} = mR(G,B)_{\text{scanned}} + b$

Table 7. Statistical summary of the differences between measured and true $L^*a^*b^*$ values (ΔE_{ab^*}) of soil samples (N=161) for different versions of the Munsell Soil Colour Chart and scanners (scanning mode, CC, rev=revised).

Scanner	Munsell Soil Colour Charts version	10R	10Y, 5GY	10YR	2.5Y	2.5YR	5R	5Y	5YR	7.5R	7.5Y, 10Y	7.5YR	Gley 1[a]	Gley 2[b]	Mean	SD
Epson V10	Japanese	2.70		2.08	1.79	2.82		1.31	2.28	5.01	1.78	2.50	2.35	4.24	2.62	1.09
	USA, rev. 1994	3.37		1.60	1.88	3.42		2.60	2.30			1.90	2.02	2.75	2.43	0.66
	USA, rev. 2009	2.78	1.96	1.30	1.79	2.93	3.15	2.97	2.11	2.70		1.46	1.42	1.59	2.18	0.69
	Mean	2.95		1.66	1.82	3.06		2.29	2.23			1.95	1.93	2.86	2.41	
	SD	0.37		0.39	0.05	0.32		0.87	0.10			0.52	0.47	1.33	0.22	
LiDE220	Japanese	2.36		2.42	1.91	2.50		2.23	2.32	3.73	2.73	2.54	3.01	5.27	2.82	0.94
	USA, rev. 1994	3.08		2.81	2.53	3.54		2.35	3.19			3.21	3.03	3.51	3.03	0.40
	USA, rev. 2009	2.18	2.22	2.24	1.86	2.28	2.93	1.84	2.17	2.17		2.36	4.14	5.13	2.63	1.00
	Mean	2.54		2.49	2.10	2.77		2.14	2.56	2.95		2.70	3.39	4.64	2.83	
	SD	0.48		0.29	0.37	0.67		0.27	0.55	1.10		0.45	0.65	0.98	0.20	
Epson V10 and LiDE220	Mean	2.74		2.08	1.96	2.92		2.20	2.40	2.30		2.30	2.66	3.75		
	SD	0.44		0.55	0.28	0.50		0.58	0.40	1.25		0.60	0.95	1.43		

[a] GLEY 1 (USA, rev. 2009): N, 10Y, 5GY, 10GY, 5G/1, 5G/2; GLEY 1 (Japanese, USA, rev. 1994): N, 2.5GY, 5GY, 7.5GY 10GY.

[b] GLEY 2 (USA, rev. 1994, rev. 2009): 10G, 5BG, 10BG, 5B, 10B, 5PB; GLEY 2 (Japanese): 5G, 10G, 5BG, 10BG, 5B, 5PB, 5P, 10RP, 5R.

SD, standard deviation.

Figure 1

Figure 2

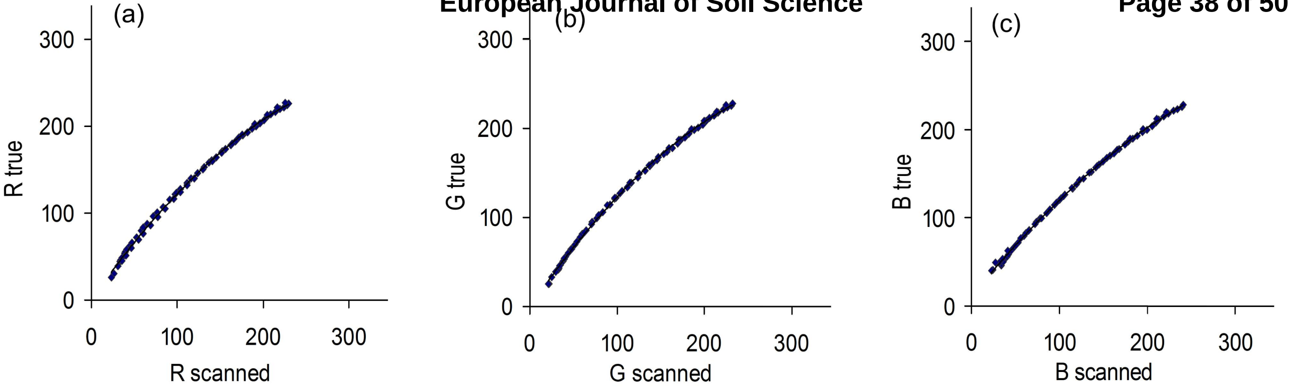

$$y = -0.0019x^2 + 1.43x - 0.22$$

$$y = -0.0019x^2 + 1.40x + 0.63$$

$$y = -0.0014x^2 + 1.23x + 10.81$$

Figure 3

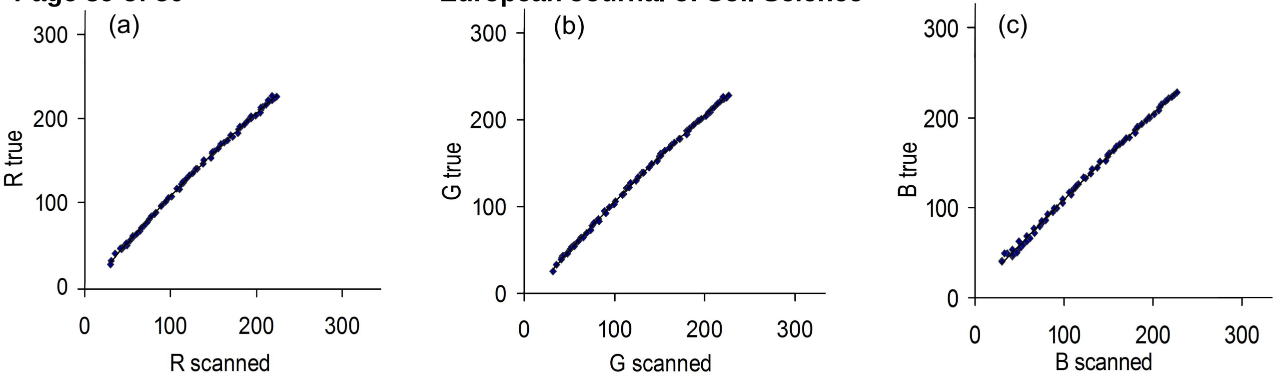

$y = -0.0008x^2 + 1.21x - 7.05$ $y = -0.0008x^2 + 1.24x - 10.98$ $y = -0.0004x^2 + 1.07x + 5.83$

Figure 4

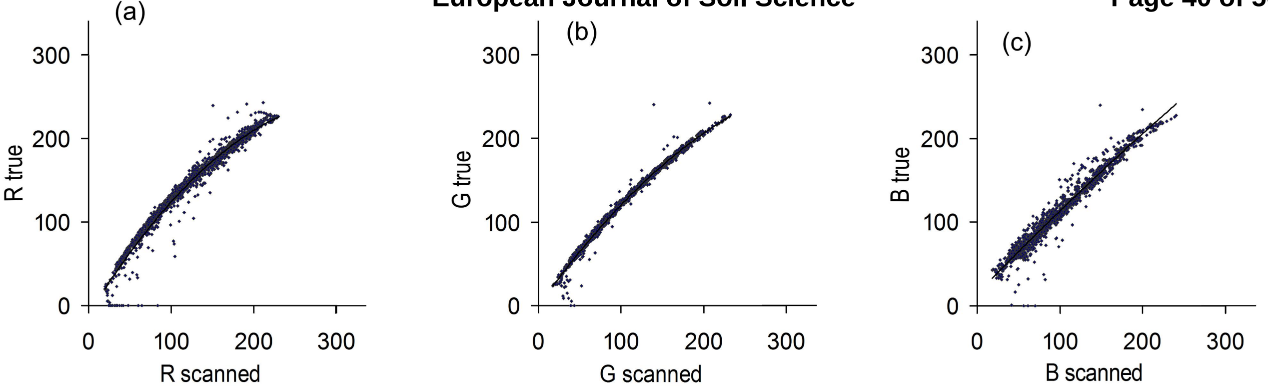

$$y = -0.0024x^2 + 1.58x - 9.87$$

$$y = -0.0017x^2 + 1.38x + 0.07$$

$$y = -0.0003x^2 + 1.02x + 14.74$$

Figure 5

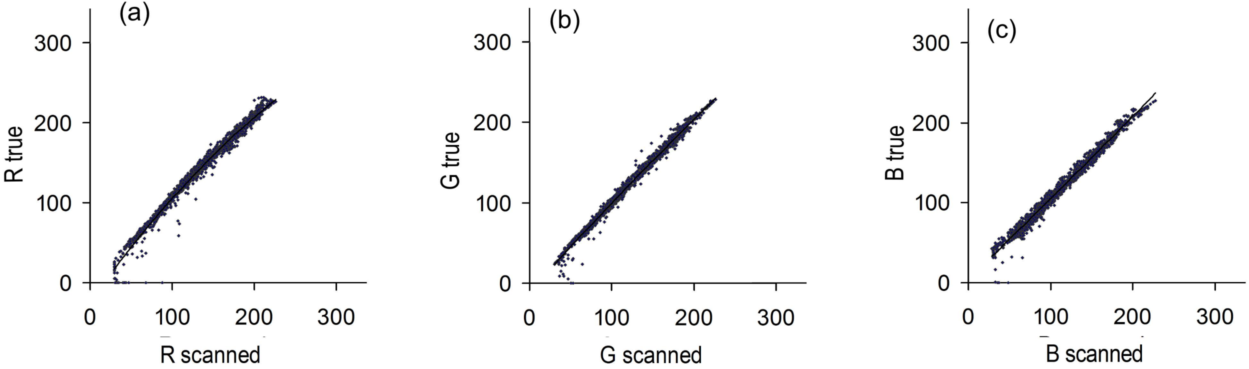

$y = -0.0013x^2 + 1.40x - 22.19$ $y = -0.0003x^2 + 1.13x - 10.59$ $y = 0.0001x^2 + 1.0x + 4.36$

Figure 6

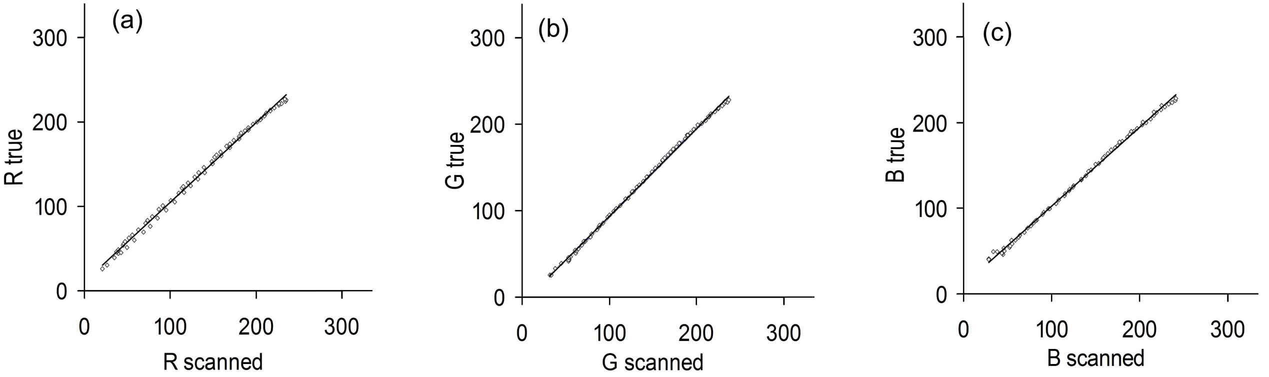

$y = 0.94x + 10.576$ $y = 1.02x - 8.01$ $y = 0.92x + 10.59$

Figure 7

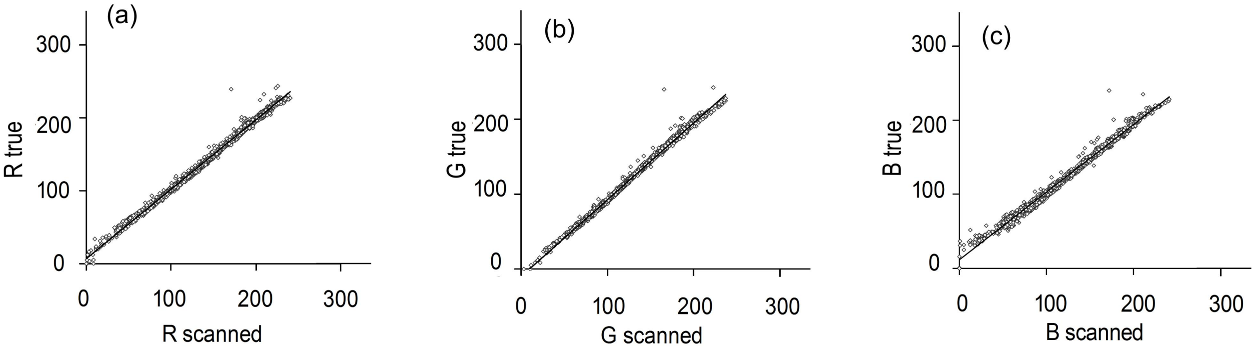

$y = 0.95x + 7.30$ $y = 1.03x - 9.62$ $y = 0.91x + 11.64$

Figure 8

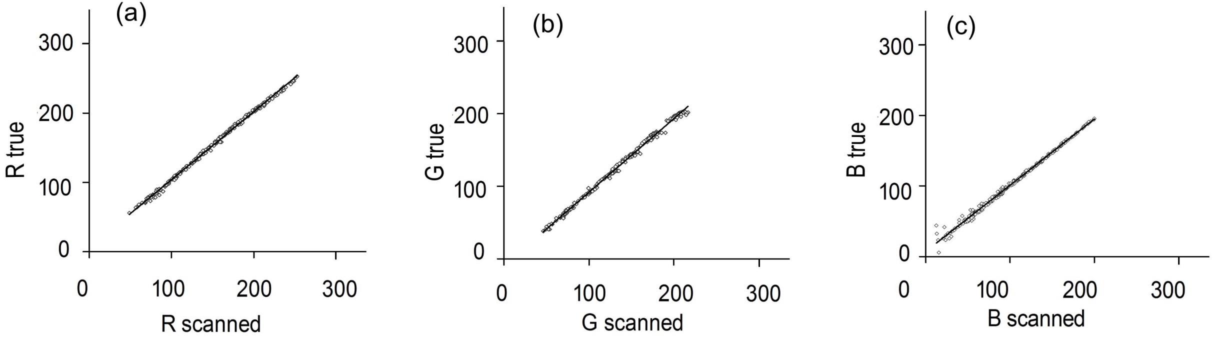

$y = 0.98x + 6.44$ $y = 1.02x - 10.44$ $y = 0.94x + 7.13$

Figure 9

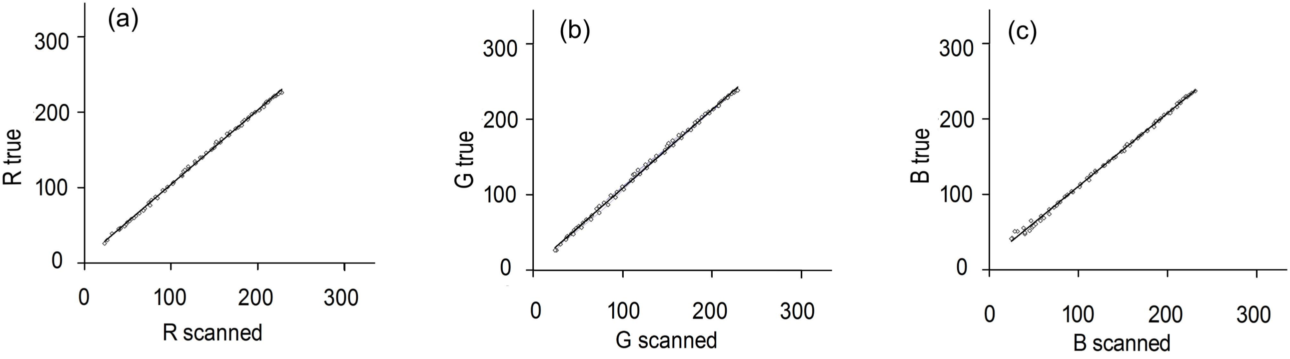

$y = 0.99x + 5.49$ $y = 1.0x + 4.50$ $y = 0.93x + 12.78$

Figure 10

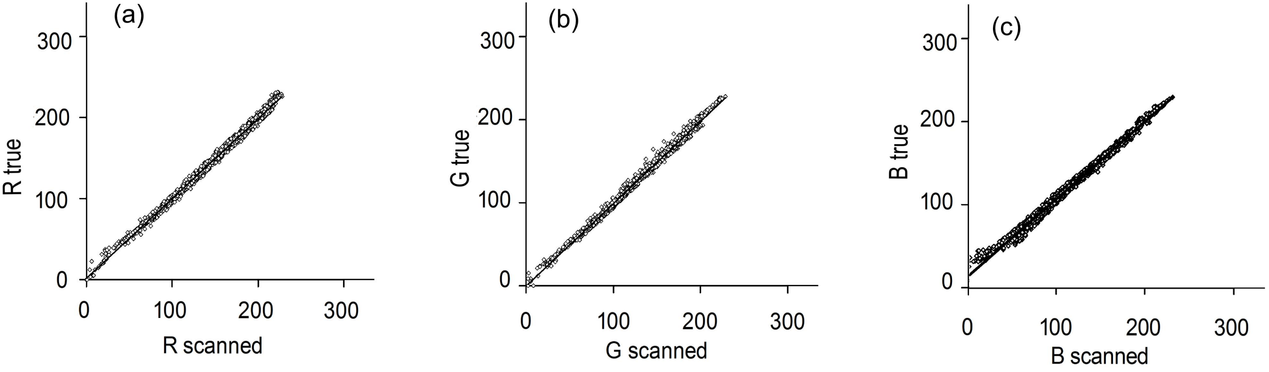

$y = 0.99x + 1.55$ $y = 0.99x - 0.18$ $y = 0.93x + 13.37$

Figure 11

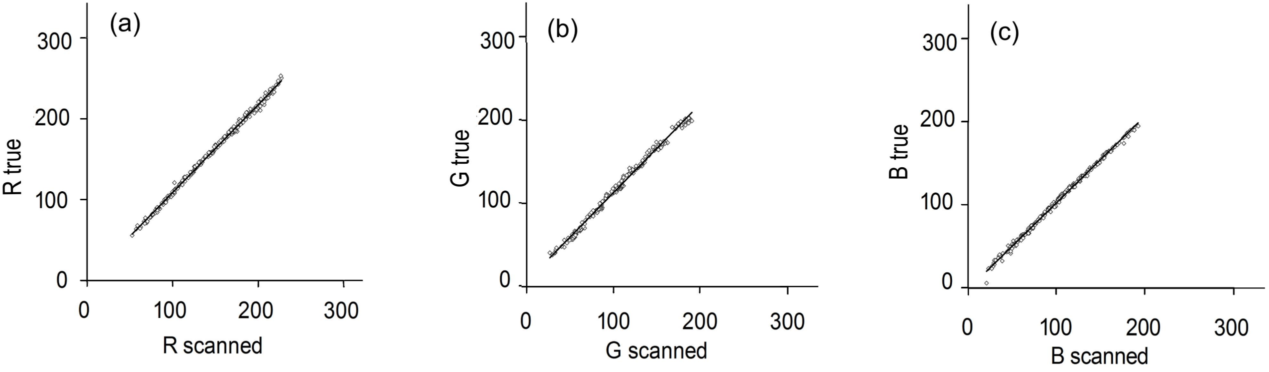

$y = 1.09x + 0.08$ $y = 1.06x + 6.09$ $y = 1.05x - 1.06$

Figure 12

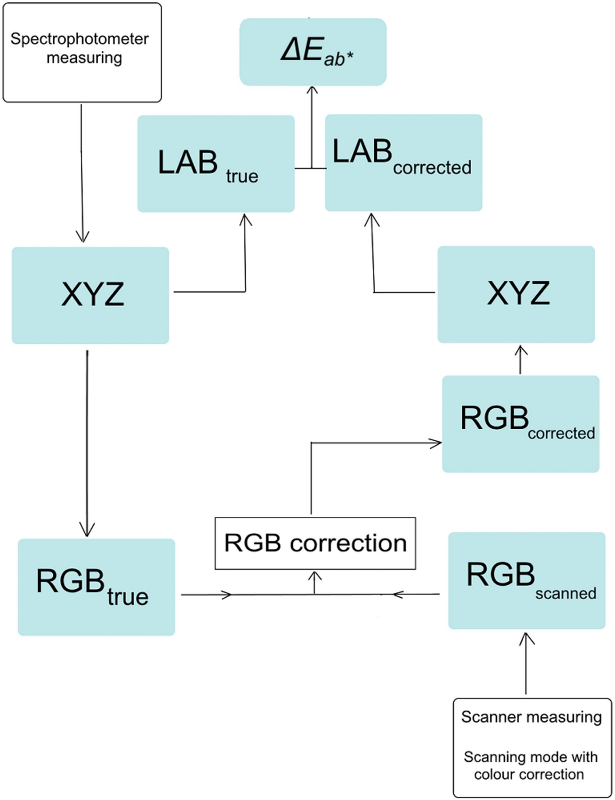
Spectrophotometer measuring
ΔEab*
LAB true
LAB corrected
XYZ
XYZ
RGB corrected
RGB correction
RGB true
RGB scanned
Scanner measuring
Scanning mode with colour correction

Figure 13

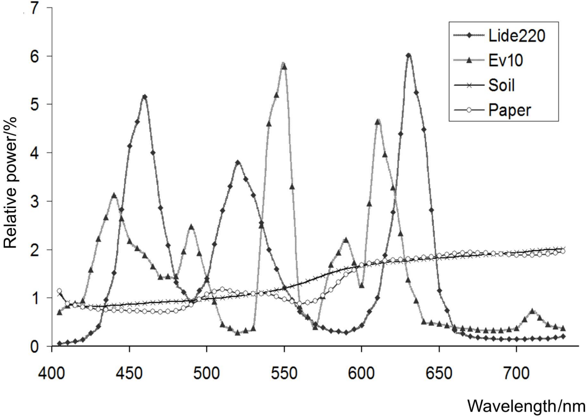
Lide220
Ev10
Soil
Paper
Relative power/%
Wavelength/nm
0
1
2
3
4
5
6
7
400
450
500
550
600
650
700

Figure 14

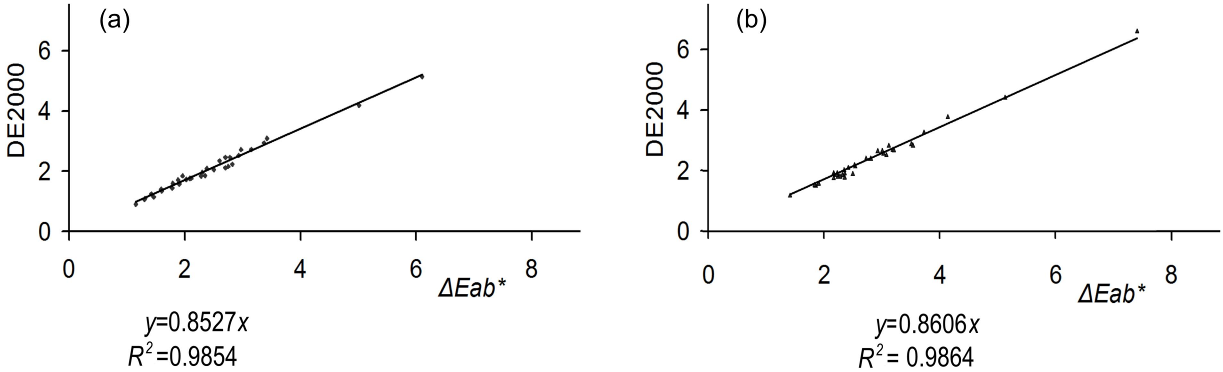
(a)
DE2000
0
2
4
6
0
2
4
6
8
ΔEab*
y=0.8527x
R2 =0.9854
(b)
DE2000
0
2
4
6
0
2
4
6
8
ΔEab*
y=0.8606x
R2 = 0.9864